Escola de Primavera de Transição e Turbulência
Blumenau 2020

12th Spring School on Transition and Turbulence
September 21st-25th, 2020, Blumenau, SC, Brazil

EPTT-2020-0030
SIMULATION OF LAMINAR-TO-TURBULENT TRANSITIONAL FLOW OVER AIRFOILS

Luís Henrique da Silva Ignacio
School of Mechanical Engineering, Federal University of Uberlândia, Av. João Naves de Ávila, 2121 Bloco 5P, Uberlândia, Minas Gerais, Brazil
luis.henrique@ifgoiano.edu.br

Carlos Antonio Ribeiro Duarte
Federal University of Goiás, Department of Engineering, Av. Dr. Lamartine Pinto de Avelar, 1120, Catalão, Goiás, Brazil.
carlosduarte@ufg.br

Francisco José de Souza
School of Mechanical Engineering, Federal University of Uberlândia, Av. João Naves de Ávila, 2121 Bloco 5P, Uberlândia, Minas Gerais, Brazil
francisco.souza@ufu.br

Abstract. *In this work, the simulation of an airfoil with NACA 63-618 cross section was performed to obtain the curves of the lift and drag coefficients as a function of the angle of attack. The interest in this profile is its application in operational current turbines, such as SeaGen, which can harness the kinetic energy of the currents of rivers and seas. A two-dimensional model was used to simulate the airfoil with a chord of 0.23 m. The Reynolds number was* $Re = 5.3 \times 10^5$ *and the angle of attack varied between* $-5^o < \alpha < 15^o$*. The values obtained were compared with experimental tests and other simulations. Several conventional RANS turbulence models have been applied, such as k-*ϵ*, optimized k-*ϵ*, SST and RSM, however none of them presented results that were in accordance with the literature. The Transition SST model showed better agreement with the experiments. It was demonstrated in the present study that the Transition SST model is fundamental in this specific case. This happens because there is a laminar-turbulent transition on the airfoil. Therefore, computational fluid dynamics (CFD) models accurately simulate provided appropriate numerical techniques are employed.*

Keywords: *airfoil, NACA 63-618, lift, drag, Transition SST*

1. INTRODUCTION

More than 5000 years ago, in the Mediterranean region, has been documented that it was probably the first device that used the wind force: the sailing ships (Singer *et al.*, 1954, 1956). Another mechanism that deserves mention is the windmill, which had its first mention around 400 B.C. and uses the kinetic energy of the wind to rotate a shaft in order to pump water or grind grains (Freese, 1957).

However these devices already captured the energy present in the winds, the term wind turbine was not yet used. This nomenclature was only applied after the Scotsman James Blyth in 1887 built a device that extracted energy from the winds with the objective of generating electrical energy, storing it in accumulators and using it to light lamps (Sørensen, 2016). Figure 1-a presents the turbine proposed by Blyth with some improvements compared to the first, for example applying metallic materials in the structure and "blades" (Price, 2005). After the success, he installed a bigger and better version of his turbine on the Montrose Lunatic Asylum, shown in Fig. 1-b (UoE, 2018).

The 1930s in the United States, wind turbines produced by Jacobs Wind Electric Company were used to supply electricity to farms and to charge batteries. Later they fell into disuse because the energy generated by fuel has become economically more advantageous (Sørensen, 2016).

Some decades ago, there was a new change in this concept/trend (Luguang and Li, 1997; Erdinc and Uzunoglu, 2012). Many works aim to supply the need to find new sources of energy and to improve the efficiency of the existing ones, since the energy generation using only fossil fuels will not supply the global demand and its burning produces undesirable gases (greenhouse effect) (Ferreira *et al.*, 2018; Jacobson *et al.*, 2018). These characteristics of fossil fuels motivate studies to focus on clean and renewable energy sources. It is important to note that renewable energy is that generated from resources that are naturally replenished in a shorter period than the human life (Frewin, 2020). Examples

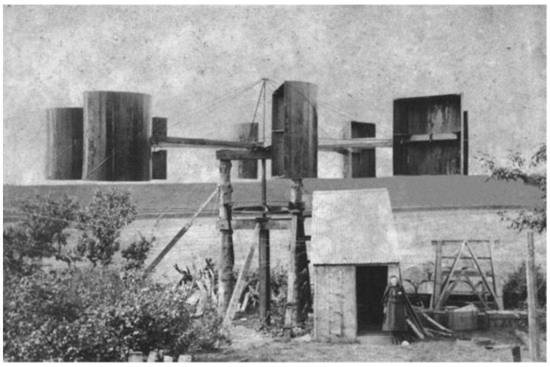

(a) James Blyth's wind turbine (Price, 2005).

(b) Turbine for the Montrose Lunatic Asylum (UoE, 2018).

Figure 1. Wind turbines by James Blyth.

of renewable energy sources include sunlight, wind, biomass and water currents (rivers, lakes and ocean) (Ng *et al.*, 2013). As an example, it is estimated that the global tidal energy capacity is around 570 TWh/yr (Behrens *et al.*, 2012). These sources can be exploited in different ways to extract their energy. Examples are the different wind turbine models, such as the horizontal axis wind turbines (HAWT) and vertical axis wind turbines (VAWT).

The basic principle of wind turbines is the friction generated between the blades and air molecules that pass around it. Currently, the blades have aerodynamic profiles. Thus, when there is a flow, an aerodynamic force is generated that can be decomposed, in relation to the flow direction, in the parallel (lift) and perpendicular (drag) directions, as shown in Fig 2.

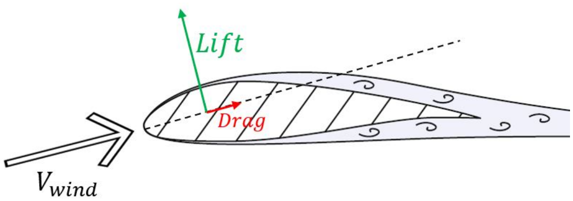

Figure 2. Forces generated in an aerodynamic profile.
(Branlard, 2017) - adapted

Wind and current turbines are very similar because both convert the kinetic energy present in a fluid into electricity (Rahimian *et al.*, 2017; Seng *et al.*, 2009). Although they are quite similar and much of what has already been developed for a wind turbine can be applied to the current turbine, it is important and necessary to specifically study each type of turbine (Walker *et al.*, 2014). It is essential to assess the performance of energy generation mechanisms for its development and improvement. In the case of these turbines, this assessment is usually modeled by means of computational fluid dynamics (CFD) or blade element momentum theory (BEM). CFD provides a greater level of detail of the interaction between the fluid (water, air) and the structure (turbine) which allows a more meticulous analysis, but involves a higher computational cost that has been mitigated with the computers progress (Rahimian *et al.*, 2017; Noruzi *et al.*, 2015; Hall, 2012). On the other hand, BEM's main characteristic is that it is simpler to implement and use when compared to CFD (Sørensen, 2016). This methodology is also suitable for wind and current turbines (Bedon *et al.*, 2013; Baltazar and Campos, 2011).

In any simulation, it is essential to reproduce what happens in practice. All details present in the CFD will only be valid if appropriate numerical techniques are applied. The same is valid for BEM, since one of the data required for the application of the technique are the curves of litf (C_L) and drag (C_D) coefficients as a function of the angle of attack (α). Such curves can be obtained experimentally or by CFD, and the simulation is generally the cheapest option. The choice of an appropriate turbulence model for the conditions to be simulated is essential to obtain good results.

In this study, some turbulence models have been selected to simulate of airfoil with NACA 63-618 cross section in order to determine the curves: $C_L \times \alpha$ and $C_D \times \alpha$. The results were compared with experimental data in the literature.

2. METHODOLOGY

The airfoil profile used in the simulations was a NACA 63-618, shown in Fig. 3. With this profile, the authors Walker *et al.* (2014) built and performed experimental tests on a turbine that is a 1:25 scale representation of the SeaGen turbine, justifying the role of this profile. The aerofoil coordinates were obtained from AirfoilTools (2020) and is presented in

Fig. 3-(a). Figure 3-(b) shows that for the leading and trailing edge regions more points were generated, as they are regions with more complex geometry and that could affect the mesh design and consequently the simulation results. The first point on the leading edge is placed at $x = 0$ and $y = 0$.

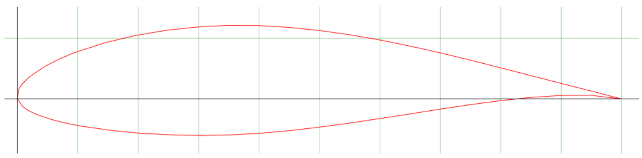

(a) Cross section (AirfoilTools, 2020).

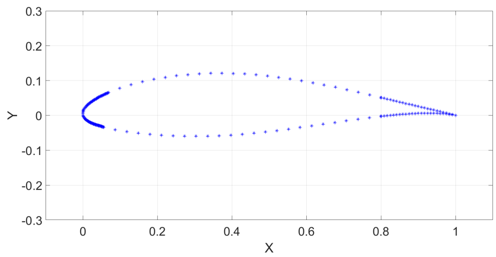

(b) Points generated.

Figure 3. NACA 63-618.

The two-dimensional mesh was generated in ICEM CFD 16.0©. Its shape and all dimensions, which are based on the chord length (C) of the airfoil, are shown in Fig. 4-(a). It is worth noting that only the vertical line downstream of the airfoil was defined as outlet (pressure outlet), and all others defined as inlet (velocity inlet). The airfoil chord is $C = 0.23\ m$ and the simulations were performed considering air as fluid ($\rho = 1.225\, kg/m^3$) with a Reynolds number of $Re_c = 5.3 \times 10^5$ in order to match the experiment of Walker *et al.* (2014). The mesh, shown in Fig. 4-(b) and (c), was developed with $y^+ = 1$ and has a total of $76,725$ elements. This number of elements provided mesh-independent results.

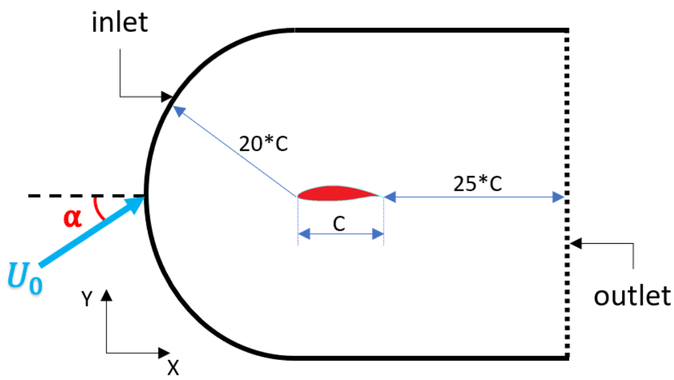

(a) Schematic representation.

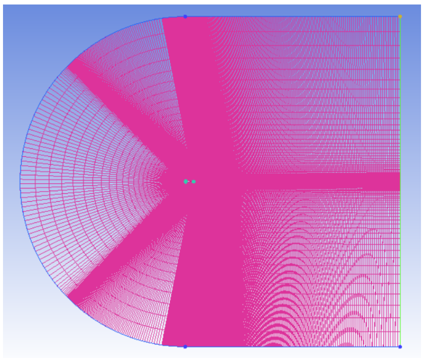

(b) Overview.

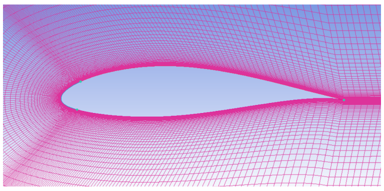

(c) Airfoil region.

Figure 4. Two-dimensional mesh for NACA 63-618.

The main objective of the present study is to compute both lift and drag coefficients by varying the angles of attack from $-5^o < \ alpha < 15^o$. For all the angles of attack, the freestream velocity $U_0 = 34.56522\, m/s$ was decomposed according to α instead of changing the position of the airfoil in the mesh (Stephens *et al.*, 2017), as shown in Fig. 4-(a). The velocity components for each angle of attack are presented in Tab. 1.

Table 1. Velocity components as a function of angle of attack.

α	$U_{0_x} [m/s]$	$U_{0_y} [m/s]$
-5^o	34.43369	-3.01256
0^o	34.56522	0.00000
5^o	34.43368	3.01256
10^o	34.04010	6.00219
15^o	33.38744	8.94613

The simulations were performed using the Fluent 16.0© and the UNSCYFL3D © code (Souza *et al.*, 2012; Pereira *et al.*, 2014). The forces F_x and F_y were oriented according to the coordinate axes shown in Fig. 4-(a). Therefore, to obtain drag and lift forces, we decomposed them to the parallel and perpendicular directions in relation to the flow direction, as shown in Fig. 2, applying the following expressions:

$$F_{Drag} = F_y \sin(\alpha) + F_x \cos(\alpha) \tag{1}$$

$$F_{Lift} = F_y \cos(\alpha) - F_x \sin(\alpha) \tag{2}$$

Once the drag and lift forces are obtained, the coefficients can then be calculated:

$$C_D = \frac{F_{Drag}}{(0.5\,\rho\,V_0^2\,C\,s)} \tag{3}$$

$$C_L = \frac{F_{Lift}}{(0.5\,\rho\,V_0^2\,C\,s)} \tag{4}$$

Since the model is two dimensional, the blade span (s) must be considered equal to the unit.

3. RESULTS

In order to obtain the values of C_L and C_D for the NACA 63-618 profile with different angles of attack and $Re_c = 5.3 \times 10^5$, simulations were carried out in Fluent 16.0© software and USNCYFL3D© code in steady-state and performing 5000 iterations. The angle of attack was varied by modifying the velocity components, as shown in Tab. 1. Note that for the same case, the results of the software and the code did not present significant difference.

An important factor, which is the central point of discussion of this work, is the different turbulence models that can be applied in the simulations. In the present study, for $\alpha = 5^o$ the conventional turbulence RANS (Reynolds Averaged Navier-Stokes) models were applied: k-ϵ, optimized k-ϵ, SST-DES (detached eddy simulation based on shear stress transport) and RSM (Reynolds stress model). However, none of them presented results in accordance with the literature: experiment $Re_c = 5.3 \times 10^5$ (Walker *et al.*, 2014) and XFoil - $Re_c = 6 \times 10^6$ (Drela and Youngren, 2006), as presented in Fig. 5. In some cases 15,000 iterations were also performed and the result for the RSM was not presented because it distorts the graph. Although the value of the Reynolds number for XFoil is higher, its results are valid for comparison, since C_L is independent of Re_c and C_D becomes independent when $Re_c \geq 5 \times 10^5$ (Walker *et al.*, 2014).

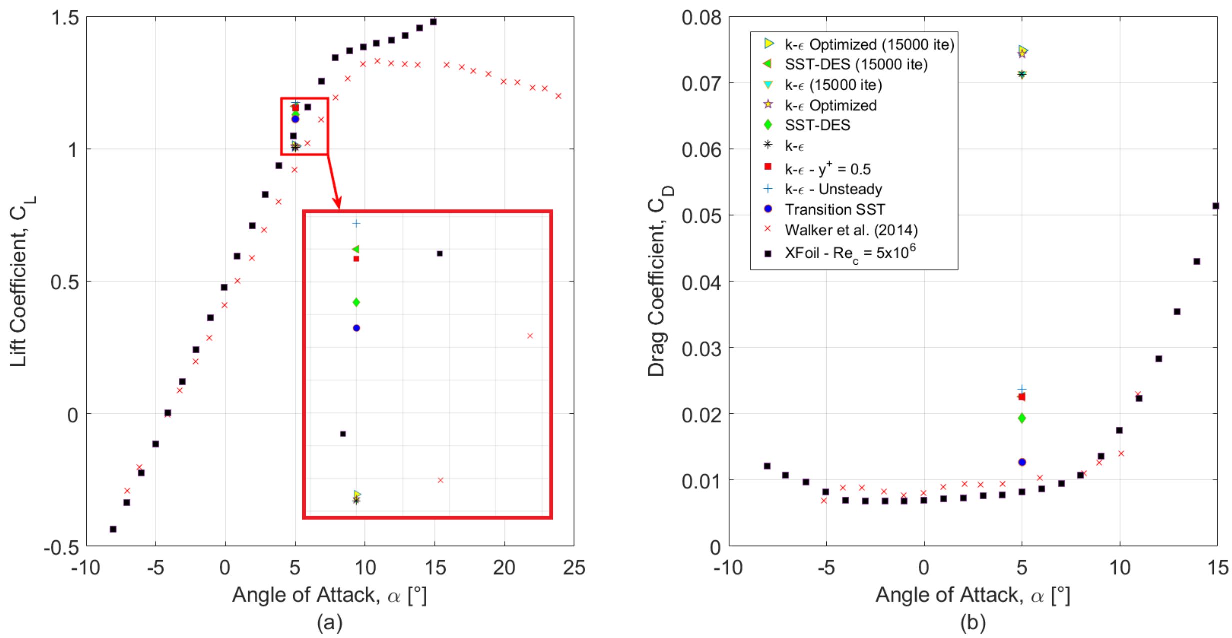

Figure 5. Lift and drag coefficients applying different turbulence models (NACA 63-618, $\alpha = 5^o$ and $Re_c = 5.3 \times 10^5$).

Studying a NACA 64-618 profile with $Re_c = 6 \times 10^6$, whose profile is very similar to that considered in this study, Han *et al.* (2018) compared the results of its simulations with different turbulence models and those experimentally obtained by Abbott *et al.* (1945), as shown in Fig. 6. The authors noted that the results for the drag coefficient with completely turbulent models show significantly high errors. The SST k-ω transition model presents a good approximation with the wind tunnel data for most angles of attack and, consequently, was the turbulence model applied in the simulations and the turbulent intensity was set as 0.01%.

Therefore, NACA 63-618 profile was performed in Fluent 16.0© for $\alpha = 5^o$ and $Re_c = 5.3\times10^5$ using the Transition SST turbulence model and turbulent intensity equal to 0.01%. The coefficients C_L and C_D obtained were closer to the references, as shown in Fig. 5-(a) and 5-(b), respectively (filled blue circle). In addition, the lift-drag ratio for this angle was also very close to the value obtained by Han *et al.* (2018), as presented in Fig. 6 (blue star).

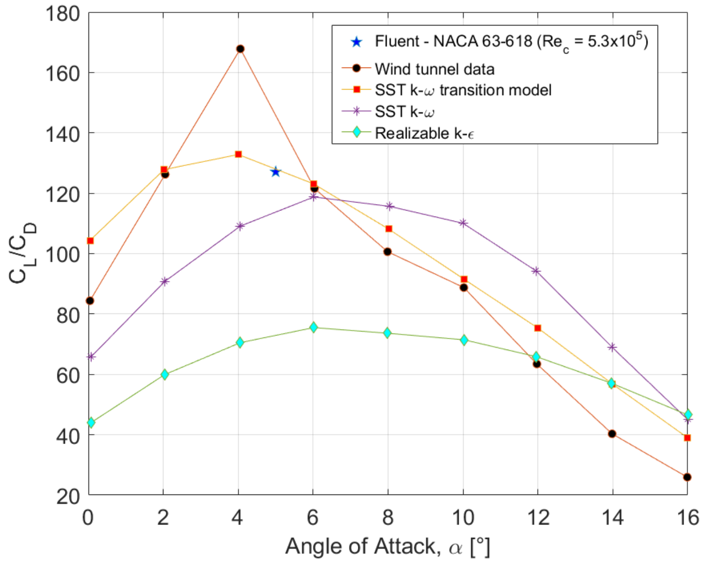

Figure 6. Lift–drag ratios in various turbulence models for NACA 64-618 and $Re_c = 6\times10^6$.
(Han *et al.*, 2018) - adapted

Based on the difference in heat transfer coefficients by convection of laminar and turbulent flows, Ehrmann and White (2015) applied infrared thermography to determine the position of laminar-turbulent transition in a NACA 63-418 profile, also very close to NACA 63-618, with Re_c ranging from 0.8×10^6 to 4.8×10^6. Figure 7 presents one of the results obtained by the authors, proving a laminar-turbulent transition on the airfoil. This laminar flow that occurs on NACA 6-series sections is one of the motivations for using them in turbines (Tangler and Somers, 1995).

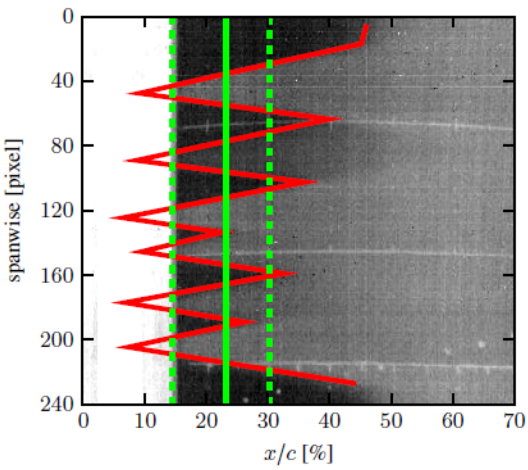

Figure 7. Red: transition front. Green: Mean (solid) and bound (dashed) locations.
(Ehrmann and White, 2015) - adapted

Finally, Fig. 8 presents the results obtained for the other angles of attack: $-5^o, 0^o, 10^o$ and 15^o, using Fluent 16.0© and applying the Transition SST turbulence model and turbulent intensity equal to 0.01%. The results are very close to references. For $\alpha = 15^o$ the C_L obtained was closer to the experimental than XFoil. The C_D is larger than the XFoil and there is no experimental data for this angle. However, Walker *et al.* (2014) shows for $Re_c = 4.2\times10^5$ and $\alpha\approx12^o$ and 13^o larger values of C_D than those obtained using XFoil, suggesting that the result obtained is coherent.

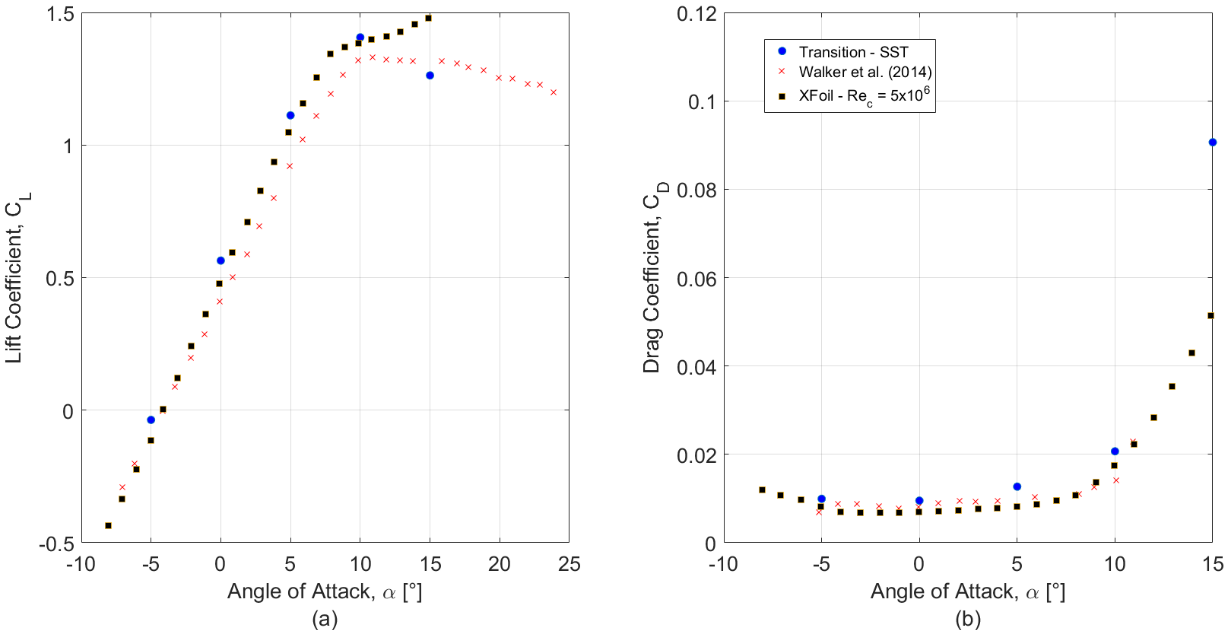

Figure 8. Lift and drag coefficients as a function of the angle of attack for NACA 63-618, $Re_c = 5.3 \times 10^5$.

4. CONCLUSION

The curves of lift and drag coefficients as a function of the angle of attack for an airfoil with NACA 63-618 cross section in the considered conditions were obtained and are in agreement with experimental values and other simulations. This result was obtained only when the Transition SST turbulence model was applied, being that the most remarkable point. Therefore, it is evident that in these conditions there is a laminar-transient transition on the airfoil.

Other studies carried out with 6-series sections also show this transition and that the use of completely turbulent models generate errors in the estimates related to the drag. As already discussed, results extracted from the CFD models will only be valid if numerical techniques are properly applied, being the turbulence model one of these techniques. Therefore, the importance of the analysis and choice of the turbulence model to be used in the simulations is highlighted, based on comparisons with experiments and simulations performed with the same or similar geometries.

5. ACKNOWLEDGEMENTS

The authors are thankful to the Coordination for the Improvement of Higher Education Personnel (CAPES), Brazilian Research Council (CNPq), and the Foundation for Research Support at Minas Gerais State (FAPEMIG).

6. REFERENCES

Abbott, I.H., von Doenhoff, A.E. and Jr, L.S.S., 1945. "Summary of airfoil data". *Report No. 824, National Advisory Committee for Aeronautics*, p. 195.

AirfoilTools, 2020. "Naca 63(3)-618". <http://airfoiltools.com/airfoil/details?airfoil=naca633618-il.

Baltazar, J. and Campos, J.F.D., 2011. "Hydrodynamic analysis of a horizontal axis marine current turbine with a boundary element method". *ASME. J. Offshore Mech. Arct. Eng.*, Vol. 133, p. 041304.

Bedon, G., Castelli, M.R. and Benini, E., 2013. "Optimization of a darrieus vertical-axis wind turbine using blade element - momentum theory and evolutionary algorithm". *Renewable Energy*, Vol. 59, p. 184–192.

Behrens, S., Griffin, D., Hayward, J., Hemer, M., Knight, C., McGarry, S., Osman, P. and Wright, J., 2012. "Ocean renewable energy: 2015–2050, an analysis of ocean energy in Australia". <www.csiro.au>.

Branlard, E., 2017. *Wind Turbine Aerodynamics and Vorticity-Based Methods*, Vol. 7. Springer International Publishing, 1st edition.

Drela, M. and Youngren, H., 2006. "Xfoil 6.96". <http://web.mit.edu/drela/Public/web/xfoil/>.

Ehrmann, R.S. and White, E.B., 2015. "Effect of blade roughness on transition and wind turbine performance".

Erdinc, O. and Uzunoglu, M., 2012. "Optimum design of hybrid renewable energy systems: Overview of different approaches". *Renewable and Sustainable Energy Reviews*, Vol. 16, pp. 1412–1425.

Ferreira, A., Kun, S.S., Fagnani, K.C., Souza, T.A., Tonezer, C., Santos, G.R. and Coimbra-Araújo, C.H., 2018. "Economic overview of the use and production of photovoltaic solar energy in Brazil". *Renewable and Sustainable Energy Reviews*, Vol. 81, pp. 181–191.

Freese, S., 1957. *Windmills and Millwrighting*. Cambridge University Press, Cambridge, 1st edition.

Frewin, C., 2020. "Renewable energy". <https://www.studentenergy.org/topics/renewable-energy.

Hall, T.J., 2012. *Numerical simulation of a cross flow marine hydrokinetic turbine*. Master's thesis, University of Washington, Washington.

Han, W., Kim, J. and Kim, B., 2018. "Effects of contamination and erosion at the leading edge of blade tip airfoils on the annual energy production of wind turbines". *Renewable Energy*, Vol. 115, pp. 817–823.

Jacobson, M.Z., Delucchi, M.A., Cameron, M.A. and Mathiesen, B.V., 2018. "Matching demand with supply at low cost in 139 countries among 20 world regions with 100% intermittent wind, water, and sunlight (wws) for all purposes". *Renewable Energy*, Vol. 123, pp. 236–248.

Luguang, Y. and Li, K., 1997. "The present status and the future development of renewable energy in China". *Renewable Energy*, Vol. 10, pp. 319–322.

Ng, K.W., Lam, W.H. and Ng, K.C., 2013. "2002–2012: 10 years of research progress in horizontal-axis marine current turbines". *Energies*, Vol. 6, pp. 1497–1526.

Noruzi, R., Vahidzadeh, M. and Riasi, A., 2015. "Design, analysis and predicting hydrokinetic performance of a horizontal marine current axial turbine by consideration of turbine installation depth". *Ocean Engineering*, Vol. 108, p. 789–798.

Pereira, G.C., Souza, F.J. and Martins, D.A.M., 2014. "Numerical prediction of the erosion due to particles in elbows". *Powder Technology*, Vol. 261, pp. 105–117.

Price, T.J., 2005. "James blyth – britain's first modern wind power pioneer". *Wind Engineering*, Vol. 29, p. 191–200.

Rahimian, M., Walker, J. and Penesis, I., 2017. "Numerical assessment of a horizontal axis marine current turbine performance". *International Journal of Marine Energy*, Vol. 20, p. 151–164.

Seng, Y., Koh, L.L. and Koh, S.L., 2009. "Marine tidal current electric power generation: State of art and current status". *Renewable Energy, InTech*.

Singer, C., Holmyard, E.J. and Hall, A.R., 1954, 1956. *A History of Technology*, Vol. 1, 2. Clarendon, London.

Souza, F.J., Salvo, R.V. and Martins, D.A.M., 2012. "Large eddy simulation of the gas–particle flow in cyclone separators". *Separation and Purification Technology*, Vol. 94, pp. 61–70.

Stephens, D., Jemcov, A. and Sideroff, C., 2017. "Verification and validation of the caelus library: Incompressible turbulence models". *ASME Fluids Engineering Division Summer Meeting*.

Sørensen, J.N., 2016. *General Momentum Theory for Horizontal Axis Wind Turbines*, Vol. 4. Springer International Publishing, 1st edition.

Tangler, J.L. and Somers, D.M., 1995. "Nrel airfoil families for HAWTs". *NREL/TP-442-7109 , National Renewable Energy Laboratory*.

UoE, 2018. "James blyth (1839 - 1906)". University of Edinburgh - 30 October 2018 <https://www.ed.ac.uk/alumni/services/notable-alumni/alumni-in-history/james-blyth>.

Walker, J.M., Flack, K.A., Lust, E.E., Schultz, M.P. and Luznik, L., 2014. "Experimental and numerical studies of blade roughness and fouling on marine current turbine performance". *Renewable Energy*, Vol. 66, p. 257–267.

7. RESPONSIBILITY NOTICE

The authors are the only responsible for the printed material included in this paper.